NODALIZATION SCHEMES FOR LUMPED-PARAMETER CALCULATIONS OF REPRESENTATIVE NUCLEAR REACTOR SEVERE ACCIDENT TESTS IN THE MISTRA FACILITY

S. Benteboula & F. Dabbene
CEA, DEN, DANS/DM2S/SFME/LATF - F-91191 Gif-sur-Yvette Cedex, France.
sonia.benteboula@cea.fr

ABSTRACT

During a severe accident involving core meltdown in a water-cooled nuclear reactor, significant amounts of hydrogen can be produced and released in the containment. The build-up of hydrogen concentrations may occur and the increase of global or local concentrations could lead to a deflagration or detonation risk which may challenge the containment integrity. Thus, extensive experimental and computational efforts have been undertaken for a better understanding of the containment thermal-hydraulics, in particular hydrogen mixing, and to evaluate the impact of mitigation means.
In this work, simulations are performed with the CAST3M-LP containment code based on two tests carried out in the MISTRA facility. These MISTRA tests are representative of a severe accident with a steam injection phase followed by nitrogen injection for inerting purpose, and finally, helium gas injection used to simulate hydrogen gas release. The two tests differ in steam and helium injection locations. Suitable nodalization schemes are elaborated to predict the containment atmosphere thermal-hydraulics and mixing. Comparisons show a good agreement between calculations and experimental results. Finally, a common nodalization scheme is proposed for the two tests and some recommendations are given to overcome the lumped-parameter method limitations.

INTRODUCTION

In nuclear reactors hydrogen can be released in the containment due to the core meltdown in severe accident situation. The hydrogen accumulation could possibly lead to deflagration or detonation under certain conditions. The assessment of hydrogen risk in the case of severe accident and the impact of the mitigation means with CFD codes could be very expensive in terms of CPU time. The use of the lumped-parameter (LP) approach, while analyzing the containment thermal-hydraulics might be more suitable for evaluation of the containment global quantities, such as pressure, due to significantly reduced computational time, if we compare it to the CFD approach. The temperature and species distribution can also be well described with the LP approach when the dominant physical process likely to take place are described with an appropriate nodalization scheme. However, this approach presents some limitations due to the fact that the local dynamics of the involved phenomena as well as the diffusive transfers are not resolved.

Separate and integral effect tests would help for the comprehension of the involved physical phenomena and to the validation of the containment CFD or LP computational codes. A set

of tests have been carried out in the MISTRA facility [1] with different geometrical configurations, injection locations and boundary conditions. The MISTRA tests used for this study, include three main phases which are representative of the containment atmosphere evolution in the case of severe accident. The first phase is the containment pressurization by the injection of superheated steam. The second phase consists in inerting the containment atmosphere by nitrogen. In the last phase helium is injected to simulate hydrogen release.

In the present work we propose some general recommendations to elaborate a multi-compartments nodalization schemes in order to carry out lumped parameter calculations and we describe how to perform a common nodalization scheme of the MISTRA geometry to simulate the different representative tests. These two tests differ from one another by the injection locations. Calculations are performed with CAST3M-LP containment code to simulate the containment atmosphere [2]. These calculations allowed to represent relatively well the experimental results and also to validate the code models.

First, a brief description of the MISTRA test facility and of the two injection tests is given. Then we describe the methodology of performing a common nodalization. Some recommendations to perform nodalization taking into account the geometry, the initial and boundary conditions are proposed for a good practice of using LP codes. Finally, the results of calculations and experiments are compared and interpreted.

1 MISTRA TESTS DESCRIPTION

1.1 MISTRA facility

The MISTRA facility is dedicated to the containment thermal-hydraulics and hydrogen risk assessment in nuclear reactors. MISTRA is a cylindrical stainless steel vessel of 97.6 m^3 (figure 1). The internal diameter of 4250 mm and the height of 7380 mm were chosen to scale a typical French PWR containment with 0.1 length scale ratio. The containment is geometrically compartmentalized by means of an inner cylinder and an annular plate. Three independent thermally regulated walls, called condensers, are inserted inside the containment, close to the external wall, on top of each other. The external wall is thermally insulated with a layer of rock wool. The space behind condensers allow fluid to penetrate and condensation may occur there due to the heat losses at the external wall. Fluid can be injected using two main lines; one is set-up at the bottom along the central axis (200 mm diameter). The second (72 mm diameter) is located just above the annular plate. In the case of spray activation, the spray nozzle is located at the top of the containment and is also used for noncondensible gas such as nitrogen injection.

1.2 TEST-1 and TEST-2 description

The tests TEST-1 and TEST-2 have been carried out to provide data for the code validation when high temperature conditions are established at the top of the containment. The tests consist of the following three phases.
(1) Steam phase: steam injection followed by a steady state defined from the balance between the injected steam and the condensed mass flowrate.
(2) Steam/nitrogen phase: nitrogen and steam injections followed by a second steady state.
(3) Steam/helium phase: helium and steam injections followed by a relaxation phase for TEST-1 and a third steady state for TEST-2.

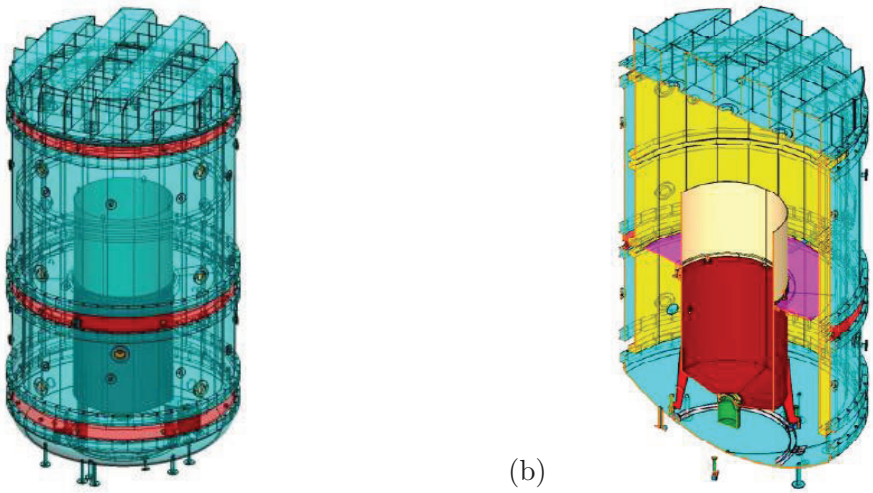

(a) (b)

Figure 1: **(a) External MISTRA containment, (b) Compartment and condensers.**

Initial homogeneous conditions are generated thanks to the preheating phase with steam injection used to heat up the steel structures in order to avoid spurious condensation on the external wall. After that, the containment is swept up with hot air to start from dry air atmosphere at the following conditions: $P_0 = 1.016\,\text{bar}$, $T_0 = 27℃$ for TEST-1 and $P_0 = 1.017\,\text{bar}$, $T_0 = 21.25℃$ for TEST-2. A main characteristic is the thermal gradient imposed on the containment regulated walls (condensers) in order to create thermal stratification. The upper condenser is maintained at 120℃ and the bottom and the middle condensers are maintained at 80℃. The initial and boundary conditions of both tests are similar, as shown in table 1, except for the injection locations of steam and helium. For TEST-1, the steam/helium upward injection is performed from the bottom of the inner cylinder, while for TEST-2, these two gases are injected in the annular space just above the annular plate. Nitrogen is injected downward from the centered nozzle located at the top for both tests. The injection conditions are summarized in table 1.

Table 1: **Injection conditions for TEST-1 and TEST-2.**

	TEST-1					**TEST-2**				
	Phase 1	**Phase 2**		**Phase 3**		**Phase 1**	**Phase 2**		**Phase 3**	
	Steam	Steam	N2	Steam	He	Steam	Steam	N2	Steam	He
Time (s)	21900	10140	3800	11160	5430	22680	10000	3800	15000	5430
Q (g/s)	80.7	80.7	25.5	80.7	2.5	79.7	79.7	25.6	79.7	2.5
T(℃)	201	201	25	205	200	187	187	21	186	200

2 MODELING AND NODALIZATION SCHEMES

2.1 MODEL DESCRIPTION

The CAST3M-LP containment code is based on a lumped-parameter formulation which consists in representing the containment free volume with a group of sub-volumes, called compartments or zones. These compartments could be in contact or not of solid walls. A sump is associated to each volume to collect condensed water or water of liquid sources. The compartments are connected to each others through atmospheric junctions and the sumps are connected through liquid junctions.

The mathematical model assumes that the flow field variables are uniformly distributed in space for each sub-volume and correspond to their average values. Thermodynamic quantities are then obtained by solving for each sub-volume the integral mass and energy conservation equations. The mass flowrate in the atmospheric junctions is determined from a simplified momentum balance equation. Heat and mass transfers on walls are given by the Uchida, Tagami or Chilton-Colburn [3] correlations for condensation ([4], [5] and [3]). These correlations rely on the wall temperature which is obtained by solving the 1-dimensional conduction equation in the wall thickness.

2.2 NODALIZATION SCHEMES FOR TEST-1 and TEST-2

Calculations have been performed with several nodalization schemes in order to reproduce quantities of interest such as the measured pressure, the wall condensation flowrates and also to investigate thermal and mass stratification through the vertical distributions of temperature and concentration for each steady state phase. Some general recommendations are established from the experience based on several validation exercises. While, for performing a nodalization scheme, one should take into account the inherent limitations of the lumped-parameters formulation such as the homogenization due to the volume averaging of the flow variables on one hand and on the other hand the local dynamics are not described. The methodology adapted is based on the analysis of the scenario characteristics such as:
- The containment geometry, by the identification of obstacles, geometrical singularities, heat and mass transfers on surfaces.
- The initial and boundary conditions.
- The injection conditions and source locations.

A preliminary step consists in calculating the homogeneous 1-compartment case. It would give information on the global containment thermal-hydraulics. The next step goal is to have a description of the spatial distribution of the flow quantities with a multi-compartments nodalization scheme according to the scenario specificity. For that, it is worthwhile to satisfy the following criteria:
- The injection zone volume should be small enough to avoid early dilution of the fluid jet.
- The atmospheric junction parameters associated to the injection compartment should be controlled in order to limit the mass flowrate in the cross direction of the inertial jet which is often overestimated. Indeed, the LP approach does not take into account the jet direction and the flow through the atmospheric junctions is due to the pressure and density differences.
- A compartment should be connected to at least two other compartments to allow fluid circulation otherwise it behaves as a dead volume. Inversely, for a dead volume, the junction parameters should be controlled to limit fluid circulation.
- To capture the pressure peaks, it is suitable to avoid the connection between the injection compartment and a condensation wall, in particular the external walls, with high thermal coefficients.
- To bring out thermal and/or mass stratification, one must have a sufficient number of compartments in the vertical direction.

The nodalization schemes shown on figures (2.a) and (2.b) are performed in light of the previous recommendations and correspond to the best-estimate calculations for TEST-1 and TEST-2. The geometrical characteristics of sub-volumes atmospheric junctions and walls exchange surfaces are determined with respect to the geometrical partitions. Sumps and liquid junctions are not taken into account in these calculations, since the condensed water is drained out of the containment during the tests.

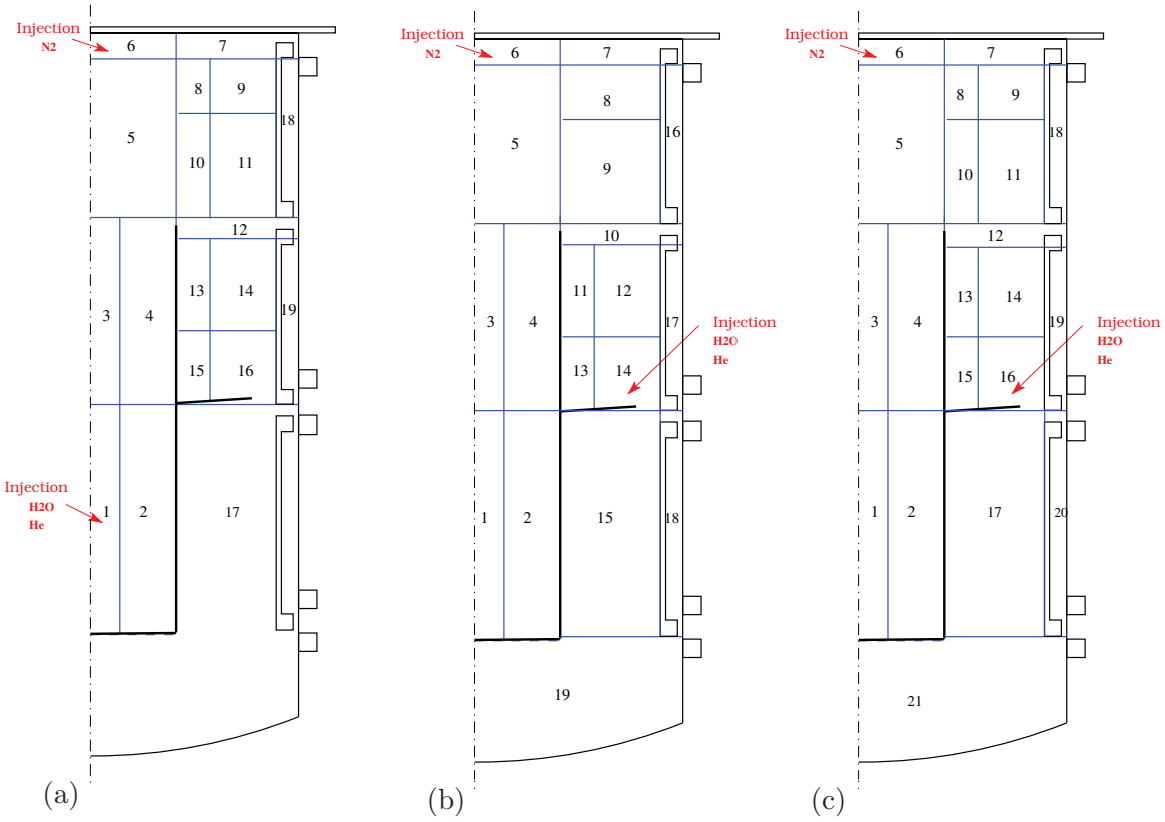

Figure 2: **(a) TEST-1: 19-compartments, (b) TEST-2: 19-compartments, (c) 21-compartments common nodalization schemes.**

TEST-1 nodalization. The compartmentalization, shown on figure (2.a), is axisymmetric and consists in subdividing the containment volume in the radial direction as follows:
1- Two rings delimited by the inner cylinder; one zone in the central part around the injection and a second adjoining zone to allow fluid entrainment in the jet thickness;
2- Two rings in the annular space above the plate to allow recirculation along the upper and middle condensers;
3- One zone behind condensers in the so-called dead-end region to allow fluid to flow behind the top and the middle condensers and to separate spurious condensation on the shell.
In vertical direction, we have:
1- Four layers in the central part with a small volume on the top to limit the nitrogen injection volume;
2- The compartment (C12) is introduced in the annular space between the upper and the middle condensers in order to reach the condensation conditions in terms of temperature and steam concentration on the top condenser by limiting the steam flowrate toward the cold condenser (middle);
3- In the annular part, three layers along the top and also three layers along the middle condenser condenser to promote condensation and the atmosphere stratification.

It should be noted that the steam and hydrogen injection inside the inner cylinder allows to avoid some specific treatment for the injection region which could be necessary in the case of the free volume tests (for more details, see [1] and [6]).

TEST-2 nodalization. Calculations showed that, the first nodalization is not appropriate for the TEST-2 which differs from TEST-1 by the steam/helium injection location performed in the annular space. Calculations revealed that the condensation mass flowrate is significantly overestimated on the bottom condenser. Therefore, some modifications have been introduced, see figure (2.b), for controlling the steam flow behind the condensers from the upper side of the annular plate, having high hot steam content, to the lower side. For these reasons, the compartmentalization is adapted in the lower part to limit the steam concentration in front of the bottom condenser.

Common nodalization. The common nodalization scheme of 21 compartments shown in figure (2.c) is a superimposition of the two previous nodalization schemes.

3 RESULTS AND INTERPRETATION

The results from analysis are based on the different steady states for each test (RP1, RP2 and RP3 refer to the first, second and third steady states, respectively). They are established when the condensation mass flowrate is equal to the constant and continuous steam injection mass flowrate.

3.1 TEST-1 results

Pressure. The computed containment pressure evolution is shown on figure (3.a). A first pressurization phase due to the steam injection followed by an almost steady state is observed. After that, the pressure increases due to inerting with nitrogen injection and a second steady state is reached. Finally, helium is released leading to a third pressurization phase. At the end of the scenario the third steady state is not reached. For instance, the condensation mass flowrate is not stabilized even if this is the case for the pressure.

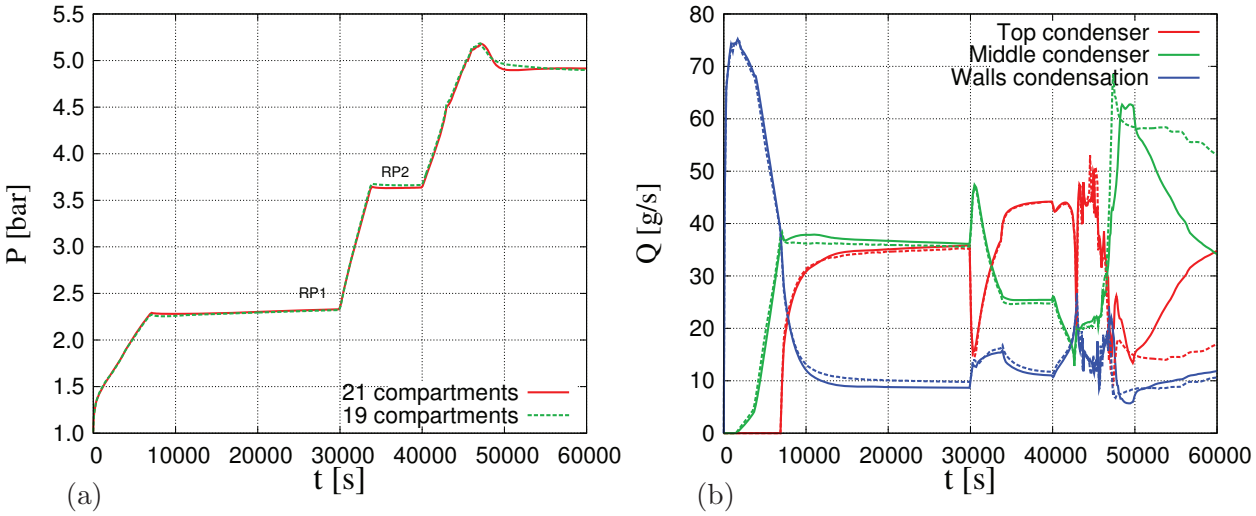

Figure 3: **TEST-1. Time evolution of the 19-compartments and 21-compartments calculations: (a) containment pressure, (b) condensation mass flowrate.**

The pressure evolutions for the two nodalization schemes are quite similar to the experimental evolution. A quantitative comparison of the pressure values for the steady states RP1 and RP2 is given in table 2.

Table 2: **Comparison between calculation and experimental results for TEST-1 and TEST-2. Containment pressure** (bar) **in the steady states.**

	TEST-1			TEST-2		
	RP1(H_2O)	RP2(H_2O,N_2)	(H_2O,N_2,He)	RP1 (H_2O)	RP2 (H_2O,N_2)	RP3 (H_2O,N_2,He)
Calculation	2.36	3.64	4.91	2.06	3.33	4.51
Experiment	2.39	3.70	4.99	2.09	3.42	4.52
Difference	1.25 %	1.62 %	1.60 %	1.43 %	2.63 %	0.22 %

Condensation rate. As shown on figure (3.b), we observe, at initial times, that the steam condensation essentially takes place on the containment wall with a high flowrate. After these times, it decreases while it starts condensing on the cold middle condenser (80°C) and just after on the hot upper condenser (120°C). At the end of the first phase ($t = 30000$ s), the condensation mass flowrate on the upper and the middle condensers are equal. In the second phase, the condensation distribution is considerably modified. At the nitrogen injection onset, the steam is instantaneously pushed down by the nitrogen injected downward from the top. This provokes simultaneous decrease of the condensation rate on the top condenser due to the enrichment with noncondensible gas, and an increase of condensation rate on the middle condenser due to the steam concentration increase. Then, the condensation rate decreases on the middle condenser due to downward motion of the nitrogen and the enrichment of this region with noncondensible gases. At the same time, the upper region is still enriched by the steam coming from the injection source which increases the condensation rate on the top condenser. In the last phase of the helium injection, a new inversion of the condensation distribution occurs but the steady state is not reached.

Table 3: **Comparison between calculation and experimental results for TEST-1 and TEST-2. Condensation mass flowrate** (g/s) **in the steady states.**

		TEST-1		TEST-2		
		RP1 (H_2O)	RP2 (H_2O,N_2)	RP1 (H_2O)	RP2 (H_2O,N_2)	RP3 (H_2O,N_2,He)
Top	calc	**35.81**	**44.18**	**6.85**	**6.55**	**5.83**
	exp	32.84	45.27	4.39	4.8	3.0
	diff	3.68 %	1.35 %	3.09 %	2.20 %	3.55 %
Middle	calc	**36.14**	**25.44**	**65.70**	**63.59**	**63.61**
	exp	33.43	17.98	62.72	59.30	61.30
	diff	3.36 %	9.24 %	3.74 %	5.38 %	2.90 %
Bottom	calc	**0.0**	**0.0**	**0.0**	**0.0**	**0.0**
	exp	2.1	2.4	0.13	0.14	1.0
	diff	2.60 %	2.97 %	0.16 %	0.18 %	1.25 %
Walls	calc	**8.67**	**11.03**	**7.13**	**9.56**	**10.22**
	exp	7.82	10.23	8.85	11.36	10.30
	diff	1.05 %	0.99 %	2.16 %	2.26 %	0.10 %
Total	calc	**80.63**	**80.66**	**79.68**	**79.69**	**79.66**
	exp	76.19	75.89	76.17	75.70	75.70

Similar evolutions of the condensation mass flowrate distribution on the different condensers and on the containment wall are obtained for the experimental and calculated results. The values of the different condensation mass flowrates obtained at the steady states RP1 and RP2 are compared to the experimental ones in table 3.

Regarding the vertical distribution of the gas temperature and concentrations, only the

21-compartments calculations are compared to the experimental results for the RP1, RP2 steady states and the post helium injection phase. The profiles are plotted for two parts, the inner cylinder ($0 \leq r \leq 0.953\,\text{m}$) and the annular region ($0.953 < r \leq 2.125\,\text{m}$).

Temperature. A thermal stratification is observed in the annular region with a high temperature layer in the upper part (beyond 5 m), and a temperature gradient of about 50°C with the lower part, as shown on figure (4.a). The temperature of the gas mixture is almost the same along the three plotted axes and is roughly dominated by the condenser temperatures. The temperature

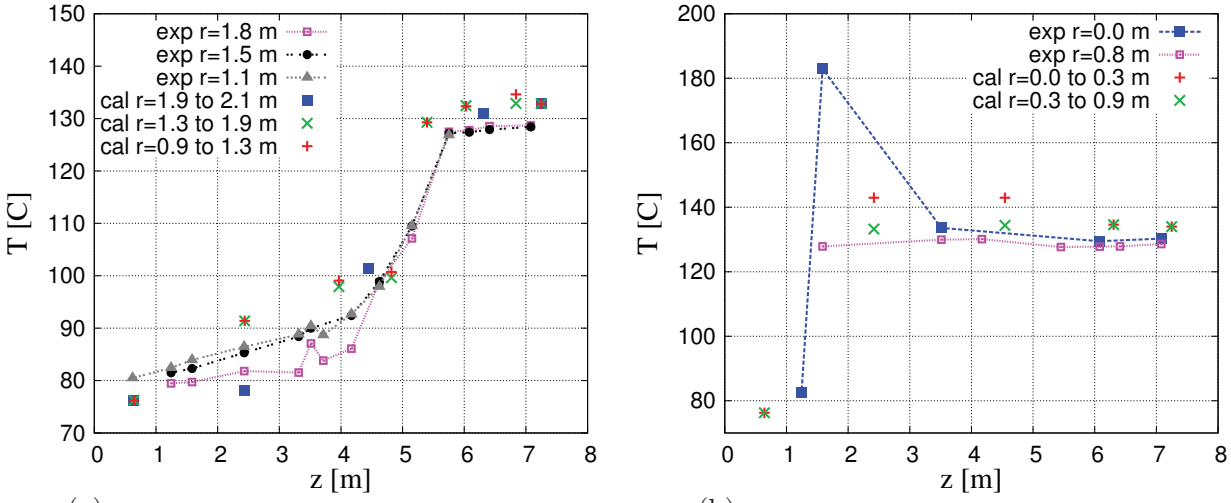

(a) (b)

Figure 4: **TEST-1. Vertical distribution of the gas temperature in the containment in the RP1 phase: (a) annular region, (b) central region.**

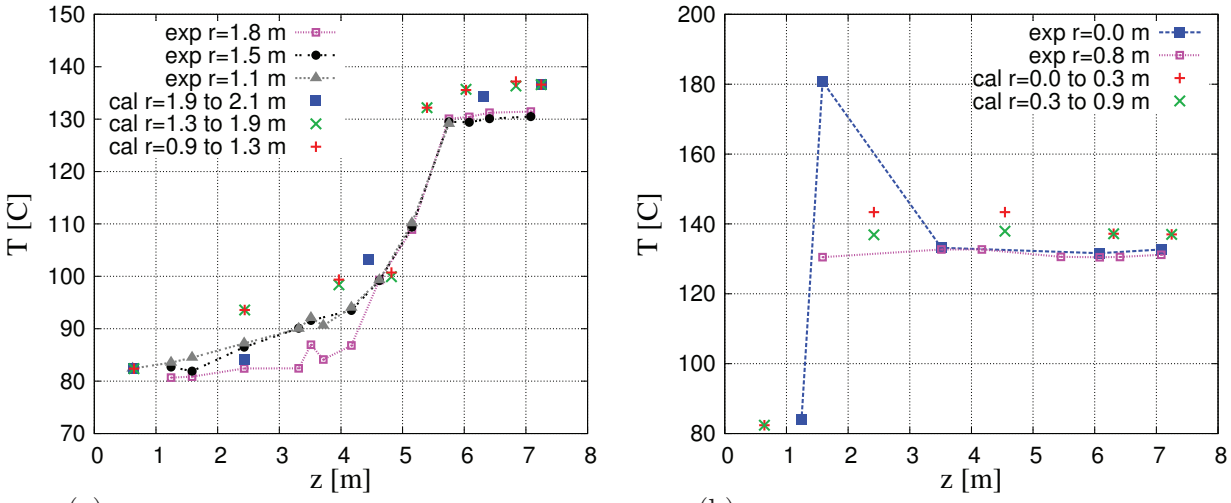

(a) (b)

Figure 5: **TEST-1. Vertical distribution of the gas temperature in the containment in the RP2 phase: (a) annular region, (b) central region.**

vertical distribution remains almost unchanged in the second steam/nitrogen steady state RP2 (see figure 5.a). In the central region, except at the lower point under the inner cylinder and at the hot

temperature point located in the steam jet axis, a thermally homogeneous hot column is observed along the axis for the two phases RP1 and RP2.

The computed results for the temperature distribution are generally in good agreement with the experimental data, especially in the steady states.

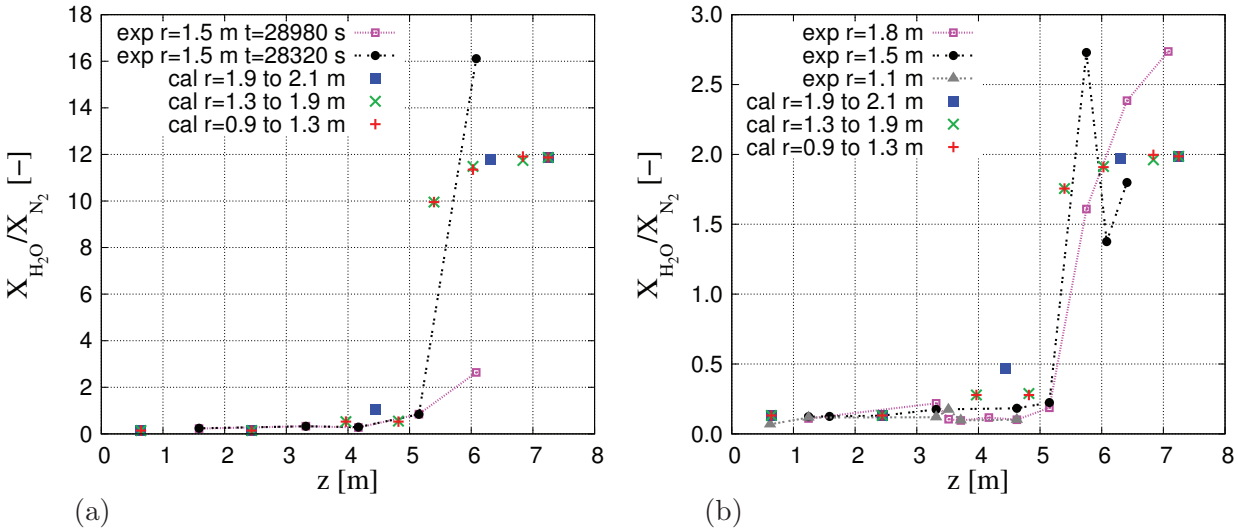

Figure 6: **TEST-1. Vertical distribution of the steam to the nitrogen concentration ratios: (a) RP1 phase, (b) RP2 phase.**

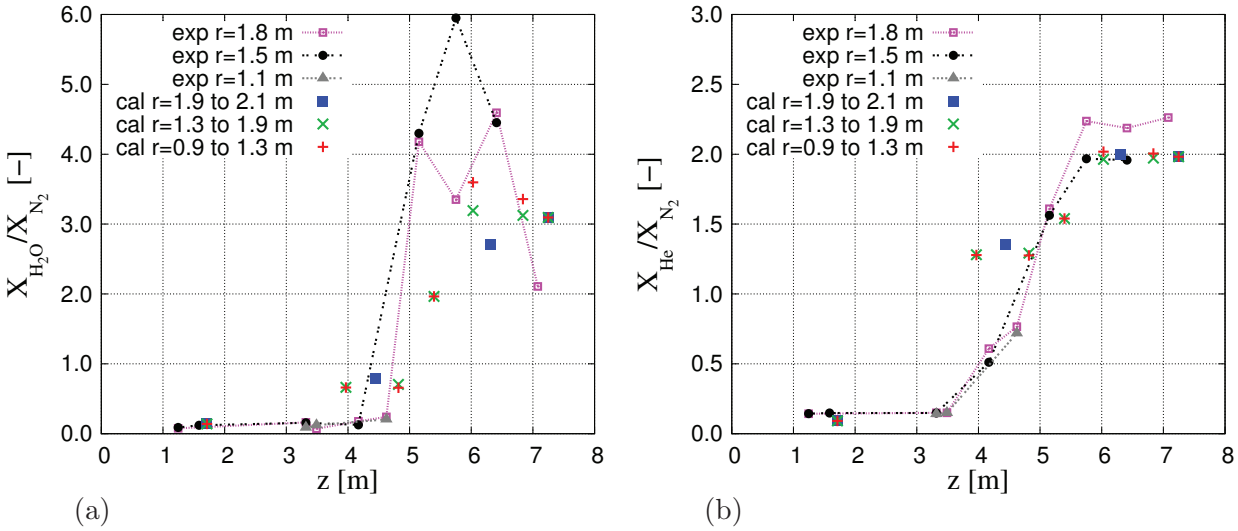

Figure 7: **TEST-1. Vertical distribution of the gas concentration ratios in the last phase: (a) steam to nitrogen ratio, (b) helium to nitrogen ratio.**

Concentration. According to the experimental data, the mixture rate is highlighted through the molar fraction ratios of the annular region. The comparison on figures (6.a) for the RP1 and (6.b) for the RP2 phases of the steam-to-nitrogen concentration ratios, shows a steam stratification on both sides of the separation (about 5 m height) with a high steam concentration layer in the upper part and high nitrogen concentration layer in the lower region. A good agreement between calculations

and results is obtained for the concentration values in the lower part as well as for the transition layer location. In the upper part, however a nearly homogeneous layer is obtained by calculations but not confirmed by the available measurements. In the last phase (figure 7), a rather good agreement is obtained for the helium concentration distribution (figure 7.b). Both experimental and computed results show steam and helium stratification with an almost homogeneous upper layer of higher He/steam concentrations and a lower layer poor with He/steam content.

3.1.1 TEST-2 results

Let us recall that in TEST-2, the steam and helium are injected in the annular space in front of the middle condenser in the upward direction (in compartment C16 on figure (2.c)).

Pressure. The evolution of the computed containment pressure is shown on figure (8.a). Compared to TEST-1, we recover the successive pressurizations and steady states but with lower values of about 0.3 bar. The pressure evolutions computed using two nodalization schemes and the experimental one are almost identical. A quantitative comparison of the pressure values obtained in the steady states RP1, RP2 and RP3 is given in table 2.

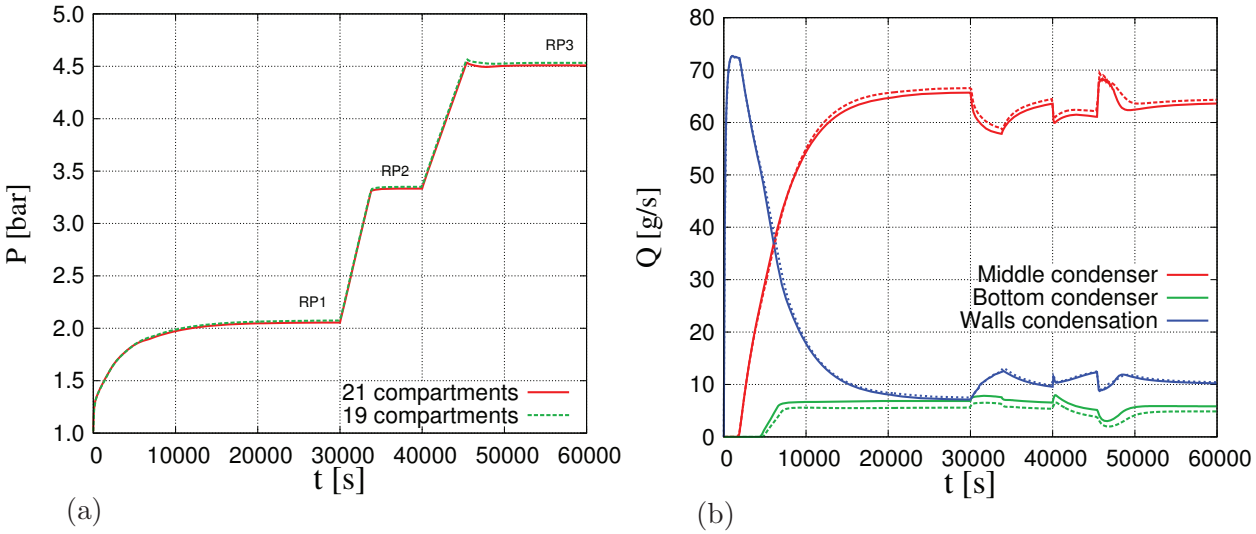

Figure 8: **TEST-2. Time evolution of the 19-compartments and 21-compartments calculations: (a) containment pressure, (b) condensation mass flowrate.**

Condensation rates. The distribution of condensation mass flowrates obtained with calculations is presented in figure (8.b). Oppositely to TEST-1, the condensation takes place only on the cold condensers (in particular on the middle condenser) all along the scenario because the steam is injected close the cold middle condenser. As a consequence, the containment pressure at the different steady states is lower than that of TEST-1 as indicated above. The time evolutions of mass condensation flowrates are similar to the experimental results on different walls. The computed values at the steady states are compared to measurements in table 3.

The mass and thermal stratifications are illustrated through the vertical distributions of temperature and species molar fractions.

Temperature. Results plotted on figures (9.a), (10.a) and (11.a) show that the 21-compartment scheme describes fairly well the local distribution of the temperature. The annular region is split up into two quasi-homogeneous parts on both sides of the ring plate; a hot upper region and a cold lower one with a temperature gradient of 35 °C. These two layers are separated with a thin layer located at 4 m height. The thermal homogenization in the upper zone is more influenced by the steam source than by the temperature gradient of condenser walls. The calculations slightly overestimate the temperature of the under-plate region. In the central zone which is less influenced by the source and walls condensation (see figures (9.b), (10.b) and (11.b)), the computed and measured temperatures are similar with a more gradual variation comparing to the annular region.

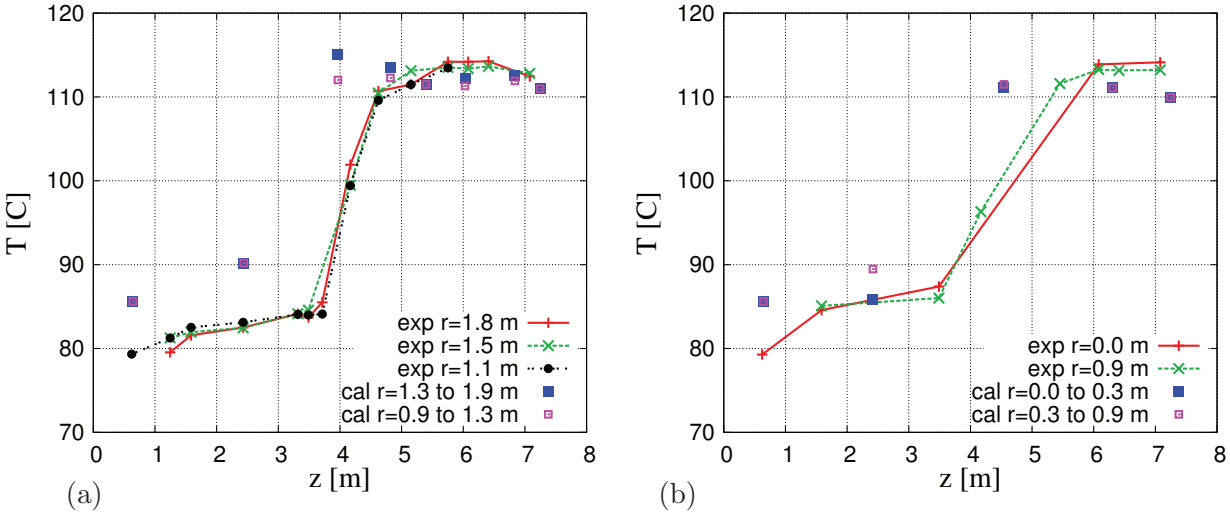

Figure 9: **TEST2. Vertical distribution of the gas temperature in the containment in the RP1 phase: (a) annular region, (b) central region.**

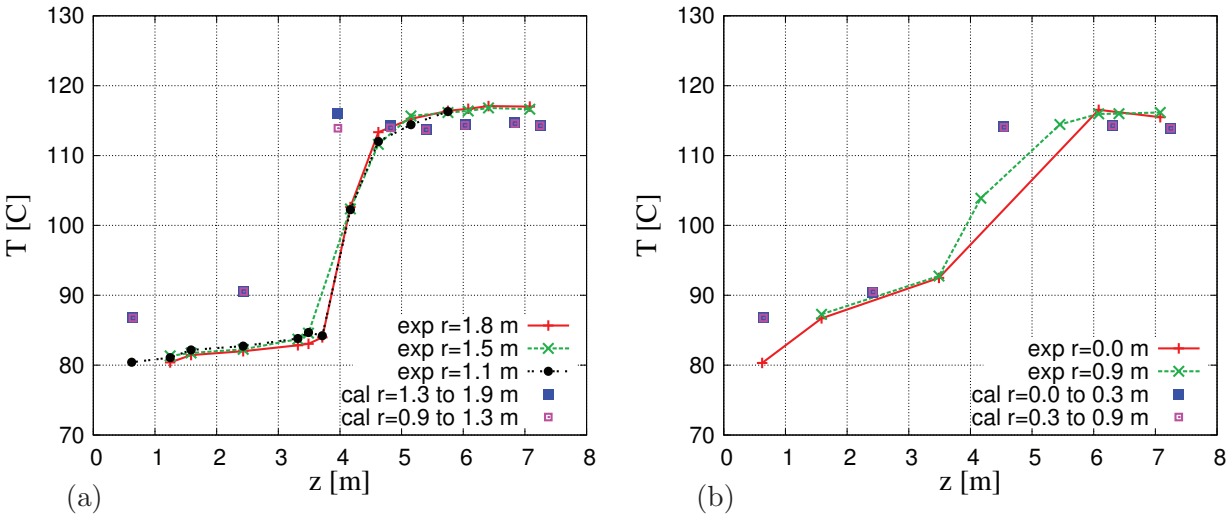

Figure 10: **TEST2. Vertical distribution of the gas temperature in the containment in the RP2 phase: (a) annular region, (b) central region.**

Concentration. On figures (12.a) and (12.b), similar to temperature distribution behavior is observed for the vertical distributions of steam and nitrogen concentrations in the annular region,

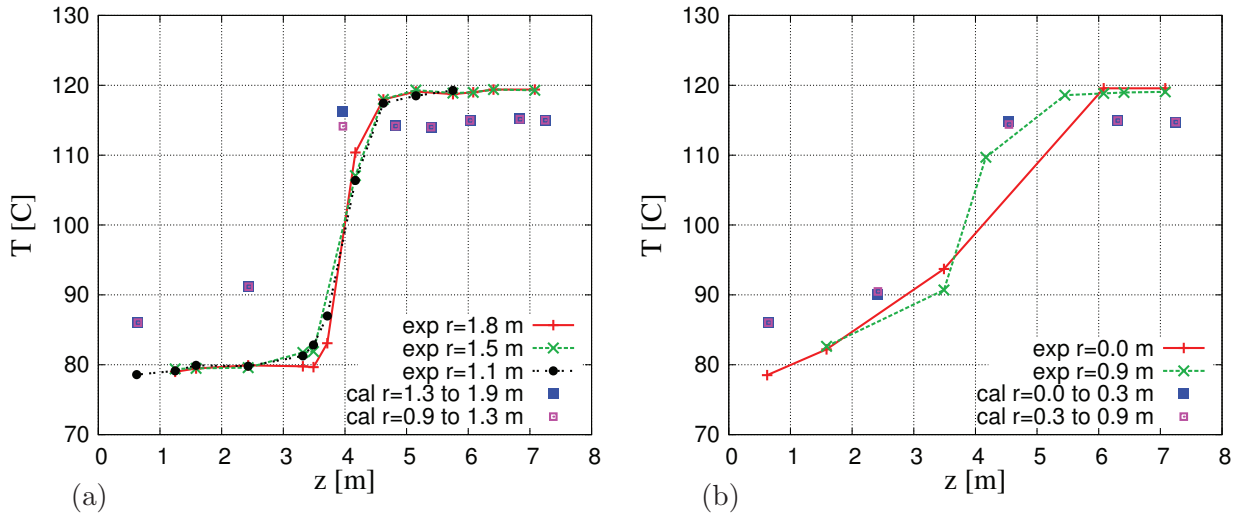

Figure 11: **TEST2. Vertical distribution of the gas temperature in the containment in the RP3 phase: (a) annular region, (b) central region.**

with a homogeneous layer having rich steam content (poor nitrogen content) above the plate and a lightly stratified layer below. Similar distribution is obtained in the second steady state RP2 with the homogenization of the lower part. The measured vertical concentration gradients between the two regions are higher than the computed gradients (see figures 13.a and 13.b). In the last phase, the flow regime was not completely steady at the measuring time. The helium injection leads to a decrease in the steam (figure 14.a) and nitrogen (figure 14.b) concentrations without modifying their vertical distributions. Nevertheless, small variation of the helium concentration with the height are observed in the annular region (figure 15.a). In the central zone (figure 15.b), Helium penetrates at middle height according to calculations. Even if the lack of measurements does not allow to precisely locate the interface, the experimental and the calculated results are quite close and a generally good agreement is obtained.

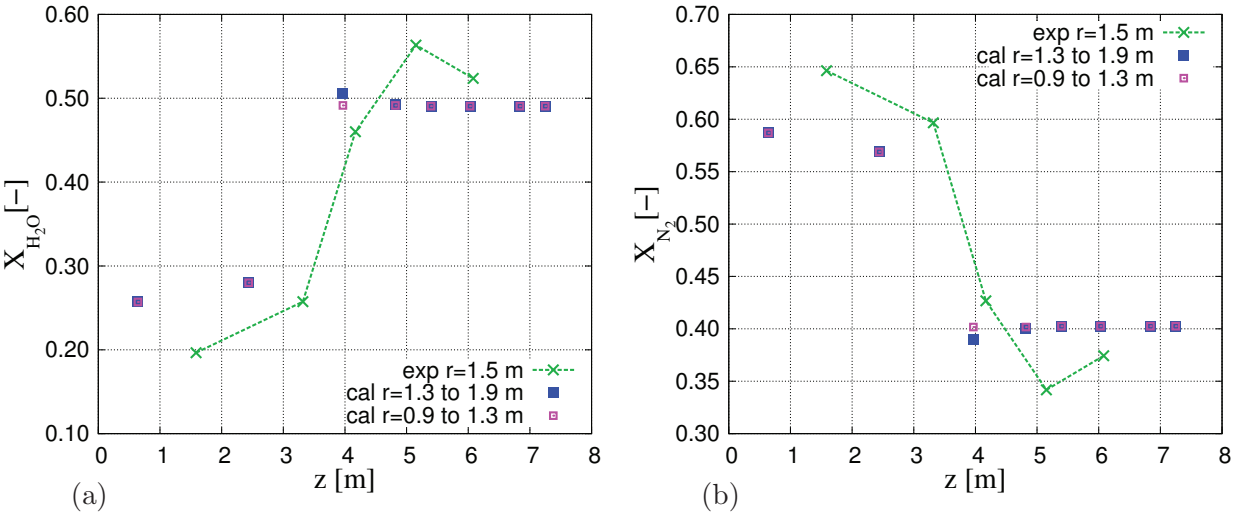

Figure 12: **TEST2. Vertical distribution of the gas molar fractions in the annular region in the RP1 phase: (a) steam, (b) nitrogen.**

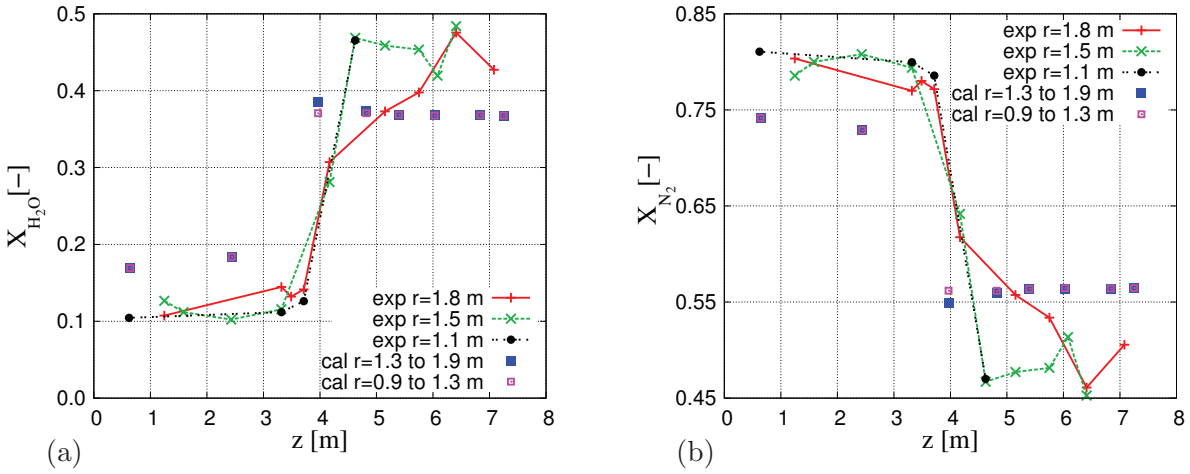

Figure 13: **TEST2. Vertical distribution of the gas molar fractions in the annular region in the RP2 phase: (a) steam, (b) nitrogen.**

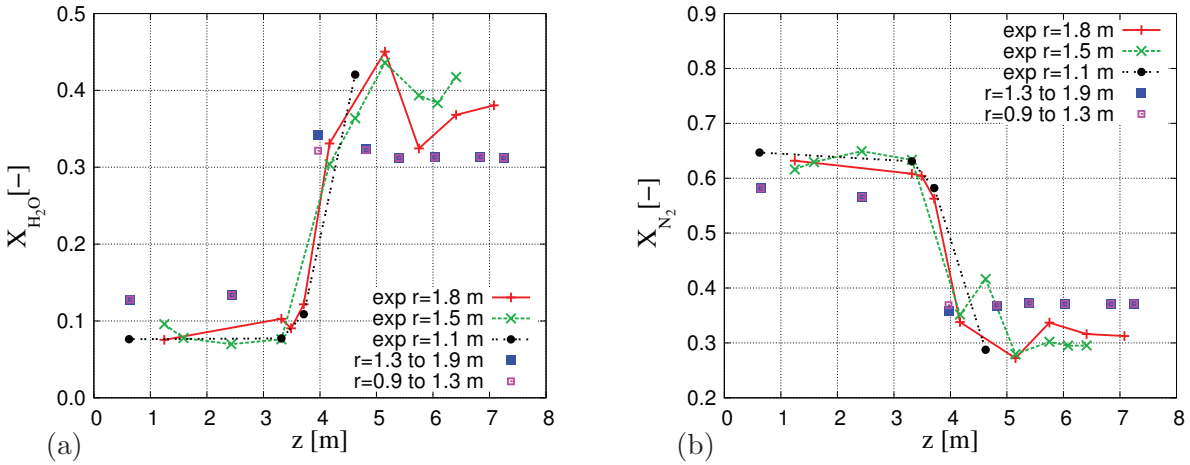

Figure 14: **TEST2. Vertical distribution of the gas molar fractions in the annular region in the RP3 phase: (a) steam, (b) nitrogen.**

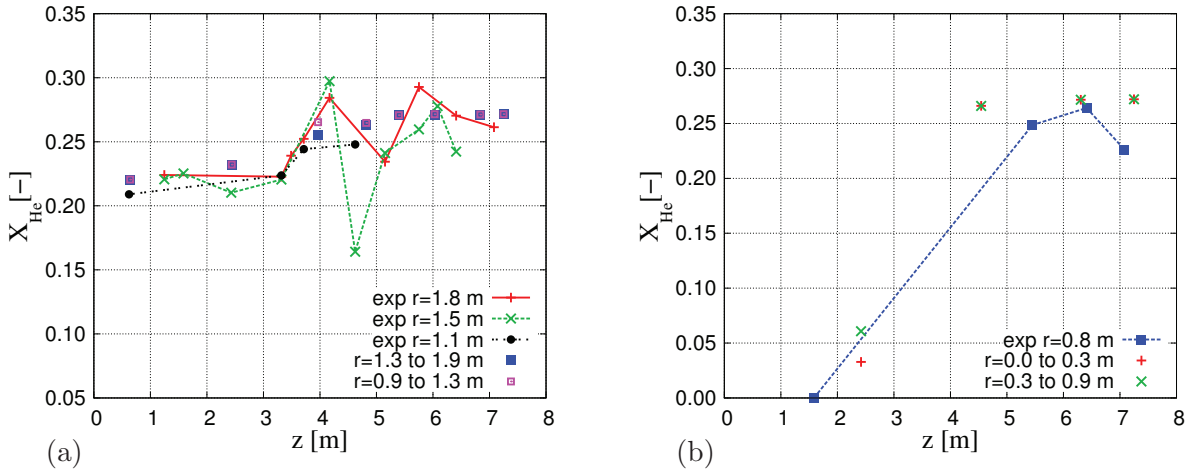

Figure 15: **TEST2. Vertical distribution of the helium molar fractions in the RP3 phase: (a) annular region, (b) central region.**

CONCLUSION

In this work, two tests performed in the MISTRA facility have been used for the validation of the CAST3M-LP containment code. The tests are representative of nuclear reactor severe accident and consist of three main phases which are the containment pressurization with steam injection, the inerting phase for the atmosphere mitigation and the helium injection used to simulate hydrogen release. They are characterized by stratifying thermal conditions on the controlled temperature walls. A thermal gradient of 40℃ is maintained between the hot upper condenser (120℃) and the two colder middle and bottom condensers (80℃). TEST-1 and TEST-2 differ from one another by the steam/helium injection locations inside the inner cylinder or in the annular space above the ring plate.

The validation is undertaken by comparing the experimental and computed quantities of interest such as the containment pressure, the distribution of condensation mass flowrate on the different walls and also the local temperature and species concentration distributions. The main feature is the appearance of an upper homogeneous layer with higher steam contents. In TEST-1, the layer is limited to the hot top condenser height where condensation also takes place. When for TEST-2, the homogeneous layer is spread out from the ring plate to the top of the containment and condensation is limited to the cold middle and bottom condensers.

The analysis of the different calculation results allowed us to develop a suitable common nodalization scheme for TEST-1 and TEST-2. It relies on the correct description of the main physical phenomena: injection, stratification, condensation, etc. which are likely to occur due to the injection sources and boundary condition effects. For that, the identification of the injection location and its link with the condensation surfaces and the geometrical singularities are key features for a better compartmentalization of the fluid volume.

References

[1] E. Studer, J.-P. Magnaud, F. Dabbene, and I. Tkatschenko. International standard problem on containment thermal-hydraulics ISP47 step 1 — results from the MISTRA exercise. *Nuclear Engineering and Design*, 237:536–551, 2007.

[2] G. Bonic and F. Dabbene. CASTEM TONUS-LP Version 2008 - Physical models. Internal report SFME/LTMF/RT/08-021/A, CEA, 2008. Internal Report DM2S SFME/LTMF/RT/04-018/A.

[3] P. Hadida. Etude du couplage des phénomènes de condensation et de conduction dans les codes 0-D, 1998. Rapport interne Quasar Informatique.

[4] H. Uchida, A. Oyama, and Y. Togo. Evaluation of post-accident cooling systems of LWR's. 93-102, 1965.

[5] H. Fujie, A. Yamanouchi, N. Sagawa, H. Ogasawara, and T. Tagami. Studies for safety analysis of loss-of-coolant accidents in light-water power reactors. *J. Japan Soc. Mech. Engrs.*, 69(571):1068–1076, 1966.

[6] M. Povilaitis, Urbonavicius E., and S. Rimkevicius. Modeling of atmosphere stratification in containements of nuclear power plants using lumped-parameter code. *Nuclear Engineering and Design*, 241:3111–3120, 2011.